# *n*-heptane hydroconversion over aluminosilicate mesoporous molecular sieves

Robert Mokaya [a,*], William Jones [a], Sonia Moreno [b] and Georges Poncelet [b]

[a] *Department of Chemistry, University of Cambridge, Lensfield Road, Cambridge CB2 1EW, UK*
[b] *Unité de Catalyse et Chimie des Matériaux Divisés, Université Catholique de Louvain, Place Croix du Sud 2/17, B-1348 Louvain-la-Neuve, Belgium*

Received 12 June 1997; accepted 30 September 1997

Aluminosilicate mesoporous molecular sieves (designated Al-MMS) have been prepared at room temperature using the primary amine hexadecylamine as organic templating surfactant. The materials have textural properties typical of mesoporous materials with short-range hexagonal order but exhibit higher Brønsted acidity compared to aluminium-containing MCM-41. The Pt-impregnated materials are efficient catalysts for the hydroconversion of *n*-heptane. At low Si/Al ratio ($\leqslant 10$) the materials have total conversions and selectivity comparable to that of USY zeolite (Si/Al = 21) and in addition exhibit considerable cyclisation at temperatures above 350°C. Our catalytic results show that the Pt-impregnated Al-MMS samples attain a good balance between the metal and acidic functions and that activity and selectivity are dependent on the Brønsted acid content and consequently on the amount of tetrahedral aluminium in the catalysts. The amount of Pt (in the range 0.25–1 wt%) mainly affects the selectivity to cyclised products which increases with Pt content at the expense of cracking; total conversion and selectivity to isomers remain largely unaffected.

**Keywords:** aluminosilicate Al-MMS, primary amine, acidity, catalytic activity, *n*-heptane hydroconversion

## 1. Introduction

The rapid phase out of lead additives has led to the search for alternative means of increasing the octane number of transportation fuels. This may be achieved by transforming straight chain alkanes into branched isomers and/or aromatics which have higher research octane numbers (RON); for example the RON of *n*-heptane is 0 compared to 56, 92 and 120 for 3-methylhexane, 2,3-dimethylpentane and toluene respectively [1]. The hydroconversion of *n*-alkanes is achieved over bifunctional catalysts consisting of noble metal particles supported on a matrix which contains Brønsted acid sites. During the reaction the noble metal catalyses hydrogen transfer reactions (hydrogenation–dehydrogenation) while isomerisation and cracking of the hydrocarbon skeleton occur on Brønsted acid sites. For a catalyst where the metal and acid functions are well-balanced, isomerisation and cracking are consecutive reactions and the rate-limiting step is the skeletal rearrangement on Brønsted acid sites of the alkenes obtained via dehydrogenation by metal sites. As far as the increase in octane number is concerned isomerisation and cyclisation are the desirable reactions while hydrocracking and hydrogenolysis are undesirable as they lead to excessive quantities of light alkanes and coke [1]. Zeolites impregnated with Pt or Pd afford high isomerisation selectivity at medium conversion levels and are the most common *n*-alkane hydroconversion catalysts. Their use is, however, characterised by high hydrocracking to undesirable alkanes at high conversion levels. Here we investigate the activity for heptane hydroconversion of a new class of aluminosilicate mesoporous catalysts which achieve conversions comparable to those of zeolites but show remarkably different product selectivities especially at high conversions.

The recent synthesis of high surface area mesoporous molecular sieves (with an array of ordered uniform pores) via a self-assembly mechanism whereby surfactant micelles act as templates for inorganic framework precursors [2–4] has attracted considerable interest due to the potential use of these materials as solid acid catalysts. The first studies of the catalytic potential of such mesoporous materials as solid acid catalysts (via aluminium incorporation) were geared towards acid-catalysed reactions of large molecules which require mild acid activity [5,6]. We have recently reported the activity of aluminosilicate MCM-41 for cumene cracking [7] and the synthesis of acidic mesoporous materials, prepared using dodecylamine as template [8], which exhibit enhanced acidity and catalytic activity for cumene cracking [9]. However, few studies have so far been reported in the open literature on the use of mesoporous molecular sieves for industrially important reactions (such as the isomerisation and reforming of *n*-alkanes) which require stronger Brønsted acid sites. Here we report on the heptane hydroconversion activity of Pt-loaded aluminosilicate mesoporous molecular sieves

---

[*] To whom correspondence should be addressed.

(designated Al-MMS) which are prepared at room temperature using the primary amine hexadecylamine as template. We show that the Al-MMS materials can achieve conversions comparable to those of zeolites and in addition (depending on Si/Al ratio) afford high levels of isomerisation and/or cyclisation at high conversions. Our findings indicate that the Al-MMS materials are potentially useful as reforming catalysts. We compare the activity of Al-MMS with an ultra-stable-Y (USY) zeolite and an aluminium containing MCM-41.

## 2. Experimental

### 2.1. Synthesis of catalysts

Al-MMS$X$ samples (where $X$ is the Si/Al ratio used in the synthesis gel) were prepared as follows; aluminium isopropoxide ($Al(i\text{-}C_3H_7O)_3$ dissolved in 35 ml isopropanol) was mixed with 0.2 mol tetraethylorthosilicate (TEOS, in 80 ml ethanol) at Si/Al molar ratios in the range 40 : 1 to 5 : 1 and vigorously stirred at room temperature for 15 min. The template solution was separately prepared by dissolving 0.05 mol hexadecylamine in a mixture of 80 ml water and 120 ml ethanol. The TEOS/$Al(i\text{-}C_3H_7O)_3$ mixture was added to the template solution under vigorous stirring at room temperature. The resulting gel mixture was allowed to react at room temperature for 20 h following which the solid product was obtained by filtration, air dried at room temperature and finally calcined in air at 650°C for 4 h to yield the catalysts. The proton form of MCM-41 ($H^+$-MCM-41-$X$, where $X$ is the synthesis gel Si/Al ratio) was prepared using the method of Mokaya et al. [7]. The $H^+$-MCM-41 (bulk Si/Al = 21.5) had a surface area of 902 $m^2/g$ and pore volume of 0.71 $cm^3/g$. The USY zeolite (CBV 740, bulk Si/Al = 21) was obtained from P.Q. Zeolites. The catalysts were impregnated with a 0.05 M solution of $Pt(NH_3)_4Cl_2$ using the required volume of solution to obtain the desired Pt-loading (0.25 to 1 wt%) and dried at 60°C.

### 2.2. Catalyst characterisation

Elemental composition (via EDA analysis) was obtained using a Camscan S4 scanning electron microscope at 20 kV. The data were processed through a ZAF4 program running on a Link 860 series 2 processor. Powder X-ray diffraction (XRD) patterns were recorded using a Philips 1710 powder diffractometer with Cu K$\alpha$ radiation (40 kV, 40 mA), 0.02° $2\theta$ step size and 1 s step time. Textural properties (surface area and pore volume) were determined at −196°C using nitrogen in a conventional volumetric technique by a Micromeritics ASAP 2400 sorptometer. Before measurement each sample was oven dried at 280°C and evacuated overnight at 200°C under vacuum. The acid content of the catalysts (prior to Pt impregnation) was measured by using TPD of cyclohexylamine. The method involves thermogravimetric analysis (TGA) following adsorption of the base on the catalysts and determines the number of acid sites capable of interacting with the base after heat treatment at 250°C. The samples were exposed to liquid cyclohexylamine at room temperature after which they were kept overnight (at room temperature) and then in an oven at 80°C for 2 h so as to allow the base to permeate the samples. The oven temperature was then raised to 250°C and maintained at that temperature for 2 h. The samples were then cooled under dry nitrogen. This procedure removed all the physisorbed base and also desorbed the base from the weaker acid sites. TGA curves were then obtained for the cyclohexylamine containing samples using a Polymer Laboratories TG analyser with a heating rate of 20°C/min under nitrogen flow of 25 ml/min. For the mesoporous materials the weight loss associated with desorption of the base from acid sites occurred between 300 and 450°C, with a maxima at ca. 370°C. This weight loss was used to quantify the acid content (in mmol of cyclohexylamine per gram of sample) assuming that each mole of cyclohexylamine corresponds to one mole of protons [10,11]. Due to presumably stronger acid sites the maxima for the USY zeolite (CBV740) was higher compared to that of the mesoporous materials. For this reason a wider temperature range (280–500°C) was used to calculate the acid content for CBV740.

### 2.3. Catalytic evaluation

The catalytic tests were performed in a fixed bed microreactor operated at atmospheric pressure. Prior to catalytic testing each sample (previously impregnated with Pt and dried at 60°C) was activated at 400°C under flowing air for 2 h following which the catalyst bed was flushed with helium and the catalyst was reduced in flowing hydrogen at the same temperature for a further 2 h. The reactor was then cooled to 150°C and stabilised at this temperature. The reaction was carried out between 150 and 400°C with 200 mg of catalyst and WHSV of 0.9 g heptane/(g-catalyst h) under temperature-programmed conditions with a heating rate of 1.7°C/min. On line gas phase analysis was performed using a HP-5880 gas chromatograph equipped with a CPSil-5 capillary column which was maintained at 30°C. Conversion percentages and yields were established on the basis of carbon balance using the method detailed elsewhere [13].

## 3. Results and discussion

### 3.1. Characterisation of the Al-MMS materials

The elemental compositions, $d$ spacing and textural properties of the Al-MMS materials are shown in table 1.

Table 1
Elemental composition, *d* spacing and textural properties of the calcined Al-MMS samples

| Sample | Si/Al ratio | $d_{100}$ (Å) | Surface area ($m^2/g$) | Pore volume ($cm^3/g$) | APD [a] (Å) | $a_0$ [b] (Å) | Wall thickness (Å) |
|---|---|---|---|---|---|---|---|
| Al-MMS40 | 44.1 | 35.1 | 1165 | 0.67 | 25.1 | 40.5 | 15.4 |
| Al-MMS20 | 26.3 | 34.2 | 1050 | 0.58 | 23.7 | 39.5 | 15.8 |
| Al-MMS10 | 12.8 | 32.2 | 1104 | 0.47 | 21.2 | 37.2 | 16.0 |
| Al-MMS5 | 7.6 | 31.6 | 901 | 0.40 | 20.1 | 36.5 | 16.4 |

[a] APD = average pore diameter (determined using BJH analysis).

[b] $a_0$ = the lattice parameter, from the XRD data using the formula $a_0 = 2d_{100}/\sqrt{3}$.

The bulk Si/Al molar ratios of the samples indicate that Si and Al are incorporated into the solid framework in proportions largely dependent on the synthesis gel composition. In all cases, however, the materials are silica rich, i.e., a greater proportion of Si in the synthetic gel is incorporated into the solid product compared to Al. The *d* spacings of the samples are comparable to values previously reported for similar mesoporous materials [14–16]. The powder XRD patterns (not shown) obtained for both as-synthesised as well as calcined samples were similar to those obtained for comparable mesoporous materials [4,14–16] i.e., a single (100) peak. Materials exhibiting such single peak XRD patterns are well characterised and are known to possess short range hexagonal symmetry [17,18]. We note that as the amount of Al incorporated increases the *d* spacing reduces. The decrease in *d* spacing was accompanied with a reduction in intensity and broadening of the (100) peak which suggests a lowering of order as the amount of aluminium in the solid framework increases. A similar reduction in hexagonal symmetry has been observed for aluminosilicate MCM-41 materials [19,20].

Table 1 also gives the textural parameters of the Al-MMS samples. The surface area, pore volume and average pore diameter (APD) values obtained are consistent with those previously reported for similar mesoporous materials such as MCM-41 [2–5,21,22]. As the amount of aluminium incorporated increases the pore volume and pore size decrease while the surface area remains high and does not change in any systematic way. The decrease in pore volume and pore size is probably due to partial collapse of the structure (during calcination to remove the template) caused by the instability associated with the presence of increasing amounts of framework aluminium. Such a phenomenon is well recognised [15,19,20].

The wall thickness values obtained by subtracting the average pore diameter (APD) from the lattice parameter ($a_0$), are consistent with those previously reported for similar materials [14]. The wall thickness increases slightly with increasing amounts of incorporated Al. It is noteworthy that the wall thickness does not show a decrease even at the highest aluminium incorporation (Si/Al = 5). This is an indication that for these materials (which are prepared using hexadecylamine, a $C_{16}$ amine) the partial collapse of the structure which would be greatest at the highest aluminium contents is not very pronounced. This contrasts with the trend we have recently observed for similar materials prepared using dodecylamine ($C_{12}$ amine) in which the wall thickness increased to a maximum value at Si/Al = 20, thereafter reducing with further increase in incorporated Al [23]. It is therefore likely that the use of primary amines with longer alkyl chains yields Al-MMS materials which possess walls of greater structural stability. If we assume that partial structural collapse generates textural mesoporosity then our observation is consistent with that of Tanev et al. [14] who have shown that the use of shorter chain amines yields materials with greater textural mesoporosity while the use of longer chain amines results in materials with framework constrained mesoporosity and much less textural mesoporosity. Thus the extent to which textural mesoporosity is generated reduces as alkyl chain length of the templating amine increases.

Table 2 gives the acid content of the Al-MMS and reference materials obtained using thermogravimetric analysis (TGA) of the desorption of cyclohexylamine from the samples. The method measures the population

Table 2
Acidity and heptane hydroisomerisation of Al-MMS and reference samples. (CHA = cyclohexylamine)

| Sample | Acidity ($\mu$mol CHA [a]) | Heptane hydroisomerisation | |
|---|---|---|---|
| | | TOF [b] ($h^{-1}$) | $E_a$ [c] ($kJ\,mol^{-1}$) |
| Al-MMS40 | 210 | 0.89 | 137 |
| Al-MMS20 | 330 | 1.04 | 144 |
| Al-MMS10 | 535 | 1.61 | 142 |
| Al-MMS5 | 650 | 2.50 | 141 |
| $H^+$-MCM-41-20 | 190 | 0.69 | 115 |
| CBV740 | 170 | 20.50 | 131 |

[a] $\mu$mol of cyclohexylamine normalised per gram of catalyst at 300°C (280°C for CBV740).

[b] Turnover frequency, calculated by dividing the rate of heptane hydroisomerisation at 250°C (expressed as $\mu mol\,g^{-1}\,h^{-1}$) by the acid content ($\mu mol\,g^{-1}$) as determined by CHA (cyclohexylamine).

[c] Activation energy, obtained by applying the Arrhenius method to the experimental isomerisation rates at conversions below 5%.

of acid sites which are accessible and sufficiently strong to interact with the base after heat treatment at 250°C [23]. Due to its strong basicity, cyclohexylamine interacts with acid sites of varying strength including those that are weak. In order to exclude the weakest acid sites and therefore determine only those sites responsible for catalysis the samples were heat-treated at 250°C. It is clear from the acid content that the incorporation of aluminium into the framework generates acid sites which are able to strongly interact with the base. The number of acid sites generated increases as the amount of aluminium in the Al-MMS framework increases. For similar bulk Si/Al ratio, the acidity of Al-MMS samples is higher than that of equivalent protonic aluminosilicate MCM-41 (compare Al-MMS20 with $H^+$-MCM-41-20).

### 3.2. Catalytic activity: hydroconversion of heptane

Curves representing the conversion of heptane achieved at different temperatures over the bifunctional USY zeolite (CBV740) and the mesoporous (Al-MMS and MCM-41) catalysts are given in figure 1. The most active catalyst is the USY zeolite (CBV-740) followed by the Al-MMS samples (whose activity depends on the amount of aluminium they contain) with the MCM-41 catalyst exhibiting the lowest activity. It is worth noting that the most aluminous (Al-MMS5) sample attains conversion close to that of the USY zeolite. The Al-MMS materials are substantially more active than MCM-41 type materials; for example, over Al-MMS20, 85% of heptane is converted at 340°C, while on MCM-41-20

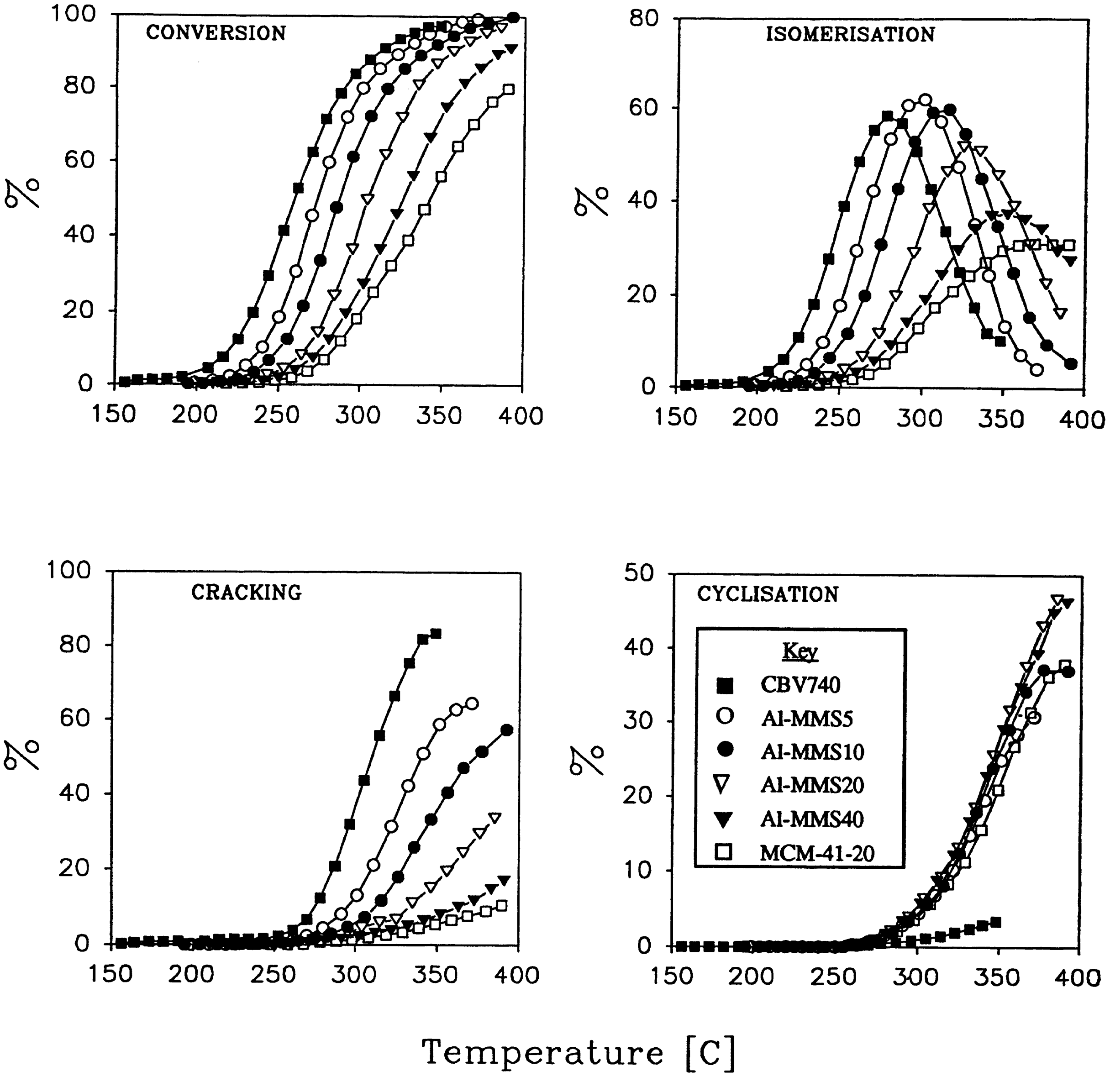

Figure 1. Heptane conversion, isomerisation, cracking and cyclisation as a function of reaction temperature. CBV-740 (■), Al-MMS5 (○), Al-MMS10 (●), Al-MMS20 (▽), Al-MMS40 (▼) and MCM-41-20 (□).

(which contains a similar amount of Al) the heptane conversion reaches only 50%. The differences in catalytic activity are more clearly illustrated by the average turnover frequency (TOF) values in table 2. The TOF values were calculated by dividing the rates of heptane isomerisation determined at 250°C (expressed as $\mu$mol $g^{-1}$ $h^{-1}$) by the acid content (expressed as $\mu$mol $g^{-1}$). For Al-MMS samples, the TOF reduces as the amount of Al decreases, suggesting that the more aluminous samples have a greater proportion of strong acid sites. The superiority of Al-MMS materials (compared to MCM-41) is apparent; the TOF of the Al-MMS20 sample is much higher than that of the equivalent (in terms of bulk Si/Al ratio) MCM-41 sample thus confirming that compared to aluminosilicate MCM-41, the Al-MMS materials possess more and stronger acid sites. The TOF of the USY zeolite is higher than that of the mesoporous materials, presumably due to its stronger acidity.

The difference in activities amongst the mesoporous materials cannot be explained by the variations in textural values which in any case decrease with increasing activity. We therefore attribute the variations in catalytic activity to differences in the acid content of the catalysts. Indeed the catalytic activity mirrors the acidity data given in table 2. This is to be expected because the bifunctional catalysts under study possess sufficient H-transfer capacity and therefore it is the amount and strength of Brønsted acid sites which are the dominant factors in controlling catalytic activity. The apparent activation energy calculated for the Al-MMS samples (using heptane conversions below 5%) do not significantly fluctuate from sample to sample. This is an indica-

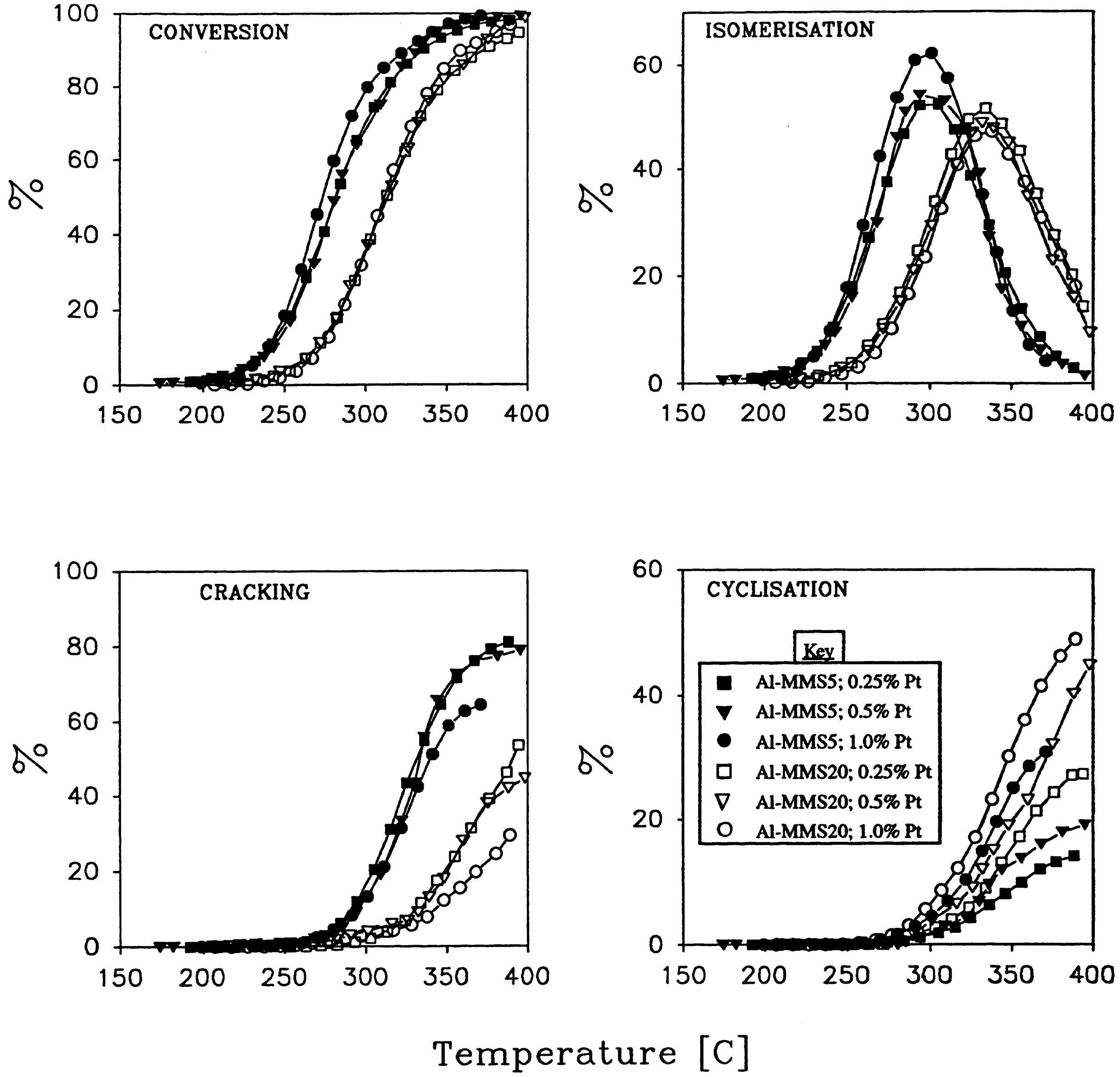

Figure 2. Heptane conversion and selectivity to isomerisation, cracking and cyclisation as a function of Pt loading for Al-MMS5 (filled symbols) and Al-MMS20 (open symbols). (●, ○) 1% Pt; (▼, ▽) 0.5% Pt; (■, □) 0.25% Pt.

tion that the reaction mechanism and the type of acid sites [24,25] involved in the reaction are the same for the different samples despite varying aluminium content. The activation energies calculated for the Al-MMS materials are comparable to that of the USY zeolite (CBV740) and are close to the upper limit of the range (125–140 kJ $mol^{-1}$) recently reported for the same reaction over a series of Pt/H-Y dealuminated zeolites [26]. The significantly different activation energy calculated for the MCM-41 sample may be an indication that this sample contains acid sites of lower strength [24].

Figure 1 also shows the percentage yields of heptane isomerisation, hydrocracking and cyclisation plotted against the reaction temperature. The catalyst type has an effect on the selectivity to isomers, cracked or cyclised products (mainly toluene). For all samples except MCM-41-20, the isomerisation curve goes through a maximum in the temperature range studied in agreement with the fact that isomerisation and hydrocracking/cyclisation are consecutive reactions. With the USY zeolite, isomerisation is the major reaction at low to medium reaction temperature; at high temperatures cracking is the main reaction. On the other hand the Al-MMS samples exhibit good isomerisation rates at low to medium temperatures while at high temperature the predominant reactions are either isomerisation, cracking or cyclisation depending on the Si/Al ratio. The higher the Si/Al ratio (and thus lower acid content) the lower the selectivity to cracking and thus isomerisation and cyclisation predominate. For the Al-MMS sample prepared at Si/Al ratio 40, (i.e., Al-MMS40) there is negligible cracking and therefore isomerisation and cyclisation are the main reactions at all temperatures. This trend is even clearer for the MCM-41 sample which has the lowest acid content amongst the mesoporous materials and as a consequence exhibits isomerisation and cyclisation with very low selectivity to cracking.

It is noteworthy that above 350°C cyclisation is a major reaction for the mesoporous materials. This high selectivity to cyclised products prompted us to investigate the effect of the Pt content on the overall selectivity of Al-MMS materials. The results are shown in figure 2 for samples Al-MMS5 and Al-MMS20. It is clear from the results that the amount of Pt on the catalysts (within the range 0.25–1 wt%) does not affect the total conversion and selectivity to isomers in any systematic way. Indeed for sample Al-MMS20 the total conversion and selectivity to isomers are virtually identical at all three Pt loadings. What emerges from figure 2 is that the selectivity to cyclised products increases with increasing Pt loading and that the increase in cyclisation happens at the expense of cracking especially at 1% loading. Remarkably isomer yields do not reduce. The increase of cyclisation at the expense of cracking at temperatures above 350°C may be explained by the consecutive nature of the hydroconversion reaction whereby isomerisation takes place at lower temperatures while both cracking (on acid sites) and cyclisation (on metal sites) are favoured at high temperature and are therefore competing reactions. The extent of cyclisation is therefore dependent on the balance between the acid and metal functions. It appears therefore that the balance attained for the mesoporous samples especially at 1 wt% Pt loading is different from that for the USY zeolite. A significant conclusion from the results shown in figures 1 and 2 is that the extent of isomerisation (the most desirable reaction) is dependent on the Si/Al ratio of the Al-MMS materials and that it varies little if at all with the Pt load-

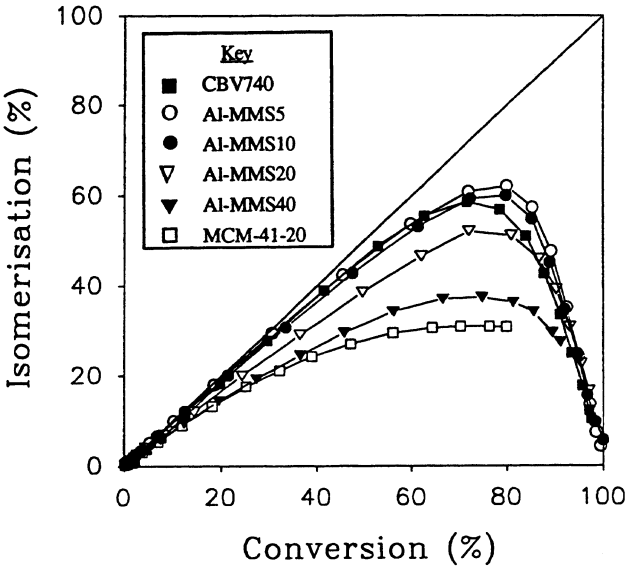

Figure 3. Yields of $C_7$ isomers vs. total conversion of heptane. CBV-740 (■), Al-MMS5 (○), Al-MMS10 (●), Al-MMS20 (▽), Al-MMS40 (▼) and MCM-41-20 (□).

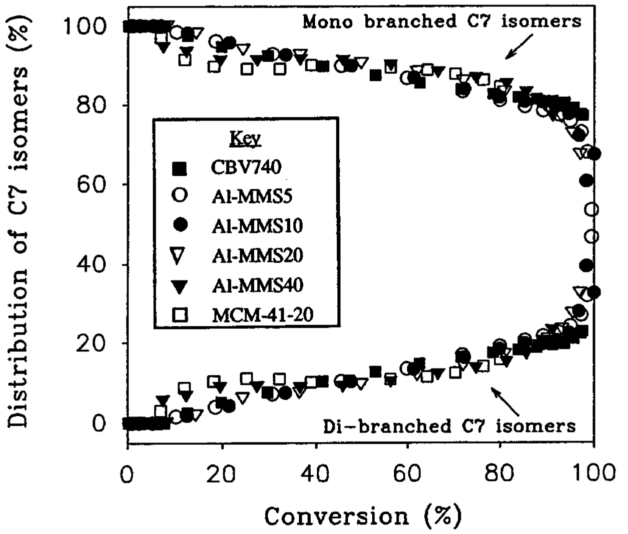

Figure 4. Variation of mono-branched and di-branched $C_7$ isomers as a function of total heptane conversion. CBV-740 (■), Al-MMS5 (○), Al-MMS10 (●), Al-MMS20 (▽), Al-MMS40 (▼) and MCM-41-20 (□).

Table 3
Yields of isomers (ISO), cracked (HC) and dehydrocyclisation (DHC) products at maximum isomerisation yield

| Catalyst | *T* Max Iso (°C) | Conv. (%) | % Yield ISO | % Yield HC | % Yield DHC | Isomerisation selectivity (%) |
|---|---|---|---|---|---|---|
| Al-MMS40 | 352 | 74.7 | 37.5 | 8.2 | 29.0 | 50.2 |
| Al-MMS20 | 325 | 72.0 | 52.1 | 6.8 | 13.1 | 72.4 |
| Al-MMS10 | 316 | 79.8 | 60.0 | 11.7 | 8.1 | 75.2 |
| Al-MMS5 | 301 | 79.9 | 62.1 | 13.3 | 4.5 | 77.7 |
| MCM-41-20 | 369 | 70.3 | 31.2 | 7.7 | 31.4 | 44.4 |
| CBV-740 | 278 | 71.5 | 58.6 | 12.4 | 0.5 | 82.0 |

ing. We further conclude that the differences in selectivity are related to the nature of the acidity on the catalysts. In samples with lower acidity, the poorer balance between the acidic and metal functions favours isomerisation at low temperature and cyclisation at high temperature. Another possible explanation of the high cyclisation may be the presence of adjacent pairs of acid–base sites on the mesoporous materials. It is possible that adjacent acid–base pairs may exist on the mesoporous samples due to the presence of extra-framework aluminium (presumably in the form of alumina which is known to possess such sites). We are currently investigating this possibility.

The variation of yields of isomers with conversion is shown in figure 3. The diagonal indicates 100% selectivity to isomers. Figure 3 illustrates the relative similarity of the most aluminous Al-MMS samples to the USY zeolite, i.e., Pt-impregnated Al-MMS5 and Al-MMS10 exhibit high isomerisation yields which are comparable to those of the Pt/USY zeolite catalyst. In addition the fact that these samples exhibit considerable cyclisation (which is negligible over the USY zeolite) makes them attractive as reforming catalysts. Figure 4 shows the variation of mono-branched (2Me-$C_6$, 3Me-$C_6$, 3Et-$C_5$) and di-branched isomers (2,3DMe-C5, 2,4DM-$C_5$, 2,2DMe-$C_5$, 3,3DMe-$C_5$) with the total conversion of heptane. The variations are the same irrespective of the sample considered and illustrate the consecutive nature of the transformation of mono-branched into di-branched isomers which is favoured at high temperature. Furthermore the fact that the isomer distribution of the mesoporous catalysts is similar to that of the USY zeolite indicates that the formation of the di-branched isomers on the zeolite is not subject to diffusional limitations despite the smaller pores in the zeolite.

In table 3 we compare the isomerisation, cracking and (dehydro)cyclisation yields obtained at the temperature of maximum isomerisation conversion (*T* Max Iso). A lower temperature at maximum isomerisation indicates greater activity and thus the zeolite which has the lowest temperature at maximum isomerisation is the most active catalyst. However, the Al-MMS catalysts attain higher conversions at maximum isomerisation. In terms of selectivity to isomers, the more aluminous Al-MMS samples (Al-MMS5 and Al-MMS10) are as efficient as the zeolite. The efficiency of the Al-MMS samples is dependent on the Si/Al ratio and thus mirrors the trend in acidity. The MCM-41 sample is the least active catalyst in terms of *T* Max Iso, total conversion and selectivity to isomers. As discussed above the less acidic Al-MMS40 and MCM-41-20 samples exhibit high selectivity to cyclisation due to poorer balance between the acid and metal functions.

## 4. Conclusions

Aluminium-containing mesoporous materials (Al-MMS) prepared using hexadecylamine (a primary amine) as organic templating surfactant have physical and textural properties similar to those previously reported for MCM-41 mesoporous materials but exhibit higher Brønsted acid content. Due to their considerable Brønsted acidity the Al-MMS materials, after impregnation with Pt, are efficient catalysts for the hydroconversion of heptane. Our catalytic results indicate that Pt-impregnated Al-MMS samples can attain a good balance between the metallic and acidic functions and that the activity and selectivity in heptane hydroconversion are dependent on the Brønsted acid content and consequently the amount of tetrahedral aluminium in the catalysts. The yields of isomers or aromatics may be optimised by changing the Si/Al ratio or in the case of aromatics the Pt loading. The combined selectivity to isomers and aromatics obtained over the Al-MMS samples is the highest we have observed for any Brønsted-acid-based catalysts and indicate the suitability of these materials as reforming catalysts.

## Acknowledgement

RM is grateful to Trinity College, Cambridge for a Research Fellowship. The assistance of Laporte Adsorbents with surface area determination is appreciated.

## References

[1] K. Tanabe, M. Misono, Y. Ono and H. Hattori, in: *New Solid Acids and Bases; Their Catalytic Properties*, Studies in Surface Science and Catalysis, Vol. 51 (Elsevier, Amsterdam, 1989) p. 303.

[2] C.T. Kresge, M.E. Leonowicz, W.J. Roth, J.C. Vartuli and J.S. Beck, Nature 359 (1992) 710.

[3] Q.S. Hue, D.I. Margolese, U. Ciesla, P.Y. Feng, T.E. Gier, P. Sieger, R. Leon, P.M. Petroff, F. Schuth and G.D. Stucky, Nature 368 (1994) 317.

[4] P.T. Tanev and T.J. Pinnavaia, Science 267 (1995) 865.

[5] J.S. Beck and J.C. Vartuli, Current Opinion in Solid State and Materials Science 1 (1996) 76.

[6] M.J. Climent, A. Corma, S. Iborra, M.C. Navarro and J. Primo, J. Catal. 161 (1996) 783.

[7] R. Mokaya, W. Jones, Z. Luan, M.D. Alba and J. Klinowski, Catal. Lett. 37 (1996) 113.

[8] R. Mokaya and W. Jones, Chem. Commun. (1996) 981.

[9] R. Mokaya and W. Jones, Chem. Commun. (1996) 983.

[10] C. Breen, Clay Minerals 26 (1991) 487.

[11] J.A. Ballantine, J.H. Purnell and J.M. Thomas, Clay Minerals 18 (1983) 347.

[12] T.R. Hughes and H.M. White, J. Phys. Chem. 71 (1967) 2192.

[13] S. Moreno, R.S. Kou and G. Poncelet, J. Catal. 162 (1996) 198.

[14] P.T. Tanev and T.J. Pinnavaia, Chem. Mater. 8 (1996) 2068.

[15] A Tuel and R. Gontier, Chem. Mater. 8 (1996) 114.

[16] T.M. Abdel-Fattah and T.J. Pinnavaia, Chem. Commun. (1996) 665.

[17] P.T. Tanev, M. Chibwe and T.J. Pinnavaia, Nature 368 (1994) 321.

[18] R. Schmidt, D. Akporiaye, M. Stocker and O.H. Ellestad, in: *Zeolites and Related Materials, State of the Art 1994*, Studies in Surface Science and Catalysis, Vol. 84 (Elsevier, Amsterdam, 1994) p. 61.

[19] Z.H. Luan, C.F. Cheng, W.Z. Zhou and J. Klinowski, J. Phys. Chem. 99 (1995) 1018.

[20] Z.H. Luan, C.F. Cheng, H-Y. He and J. Klinowski, J. Phys. Chem. 99 (1995) 10590.

[21] P.J. Branton, P.G. Hall, K.S.W. Sing, H. Reichert, F. Scuth and K.K. Unger, J. Chem. Soc. Faraday Trans. 90 (1994) 2965.

[22] J. Rathousky, A. Zukal, O. Franke and G.J. Schulz-Ekloff, J. Chem. Soc. Faraday Trans. 90 (1994) 2821.

[23] R. Mokaya and W. Jones, J. Catal. (1997), in press.

[24] A. Corma, F. Llopis, J.B. Monton and S. Weller, J. Catal. 142 (1993) 97.

[25] P.A. Jacobs, *Carboniogenic Activity of Zeolites* (Elsevier, Amsterdam, 1977) p. 139.

[26] M.J. Remy, D. Stanica, G. Poncelet, E.J.P. Feijen, P.J. Grobet, J.A. Martens and P.A. Jacobs, J. Phys. Chem. 100 (1996) 12440.